STM JOURNALS

Journal of Structural Engineering and Management
ISSN: 2393-8773(online)
Volume 1, Issue 3
www.stmjournals.com

Effect of Silica Fume and Granite Powder on the Ratio of Mode II to Mode I Fracture Energies of Steel Fiber Reinforced Concrete

***A. Sreenivasa Rao*[1]*, G. Appa Rao*[2]**
[1]Civil Engineering, RSR Engineering College, Kadanuthala, Kavali, A.P., India
[2]Structural Engg. Laboratory, Civil Engg. Dept., IIT Madras, Chennai, India

Abstract
The paper presents the results of an experimental investigation which assesses the effect of silica fume and also granite powder on fracture of steel fiber reinforced concrete under Mode I and Mode II loadings. Tests have been conducted on new notched beam specimens under pure shear (proposed in earlier paper of the authors). The test specimens made from concretes in which partial cement replacement (10%) by (1) silica fume and (2) granite powder were used. The shear fracture energy and flexure fracture energy were calculated and an attempt has been made to know the ratio of Mode II to Mode I fracture energy. With the silica fume, increase in the values of mechanical and fracture properties was observed whereas with granite powder decrease in all the values was found.

Keywords*: Fiber reinforced concrete, silica fume, granite powder, mode I failure, mode II failure and fracture toughness*

****Author for Correspondence*** E-mail: prof.asrao@gmail.com

INTRODUCTION

In an earlier paper of the authors, it was concluded that the all-round notch specimen could be successfully used for Mode II fracture [1, 2]. Further studies were conducted on the same specimens of steel fiber reinforced concrete (SFRC) in which partial cement replacement of 10% by (1) silica fume (SF) and (2) granite powder (GP) were used. The mass production of cement poses severe environmental hazards on one hand and unrestricted depletion of natural resources on the other hand. This threat to ecology has led to several investigations to utilize industrial by-products as supplementary cementitious material in making concrete. The use of cement replacement materials has beneficial environmental and production cost implications. In addition, depending on the proportions used and age of concrete, such pozzolanic materials such as pulverized fuel ash (fly ash), silica fume and metakaolin can enhance the performance of the resulting material both in terms of strength and durability. The increase in strength of concrete containing these binders is accompanied by a change in the behavior approaching that of a homogenous material with a possible increase in brittleness.

Studies were conducted to investigate the mechanical and fracture properties of SFRC under Mode II loading using a new specimen geometry and JSCE SF-6 test method of loading on the specimens of steel fiber reinforced concrete (SFRC) in which partial cement replacement of 10% by (1) silica fume (SF) and (2) granite powder (GP) were used [1–3]. In both cases, steel fibers of diameter 0.53 mm and length 25 mm with volume fractions (V_f) between 0 and 1.5% were used. All investigations were carried out using ordinary portland cement (OPC). From these test results the shear fracture energy and flexure fracture energy were found out and are compared with plain SFRC.

RESEARCH SIGNIFICANCE

The SF contains large proportions (about 90%) of extremely fine amorphous particles of silicon dioxide. In itself, SF does not have any binding properties, but it reacts with $Ca(OH)_2$

on hydration of cement and produces gel, i.e., calcium silicate hydrate which has good binding properties. This densifies the whole concrete structure resulting in increased strength and reduced permeability. Micro-silica because of its high fineness reduces bleeding so that no bleed water is trapped beneath coarse aggregate particles; chemical reaction of micro-silica results in lower porosity in the interface zone.

Even though the granite powder is not a pozzolanic material, it can be used as a filler material. Hence, its effect on performance of the resulting material shall also be studied. Several research findings were reported on the fracture behavior of concrete in Mode I loading. However, studies on Mode II loading effects are very limited for plain concrete in general and fiber reinforced concrete in particular. Investigations were reported on the effect of silica fume on the fracture behavior of fiber reinforced concrete under Mode I loading. An attempt has been made in this paper to study the effect of silica fume and also granite powder on the fracture behavior of steel fiber reinforced concrete under Mode II loading using a new specimen geometry and JSCE SF-6 test method [1–3].

LITERATURE REVIEW

High strength concrete (HSC) and high performance concrete (HPC) are considered as relatively new materials. The use of silica fume, fly ash and super plasticizer with careful selection of constituent materials has made the production of HSC or HPC easier and more beneficial. Concrete with compressive strength greater than 60 MPa is generally classified as HSC. It could be considered as HPC if other attributes are satisfactory in terms of its intended application. Low w/c (≤ 0.35) at higher cementitious content (> 500 kg/m^3) with or without supplementary materials like fly ash and silica fume, and water reducing admixtures are inevitable in HSC. Use of silica fume, as cement replacement material, has been reported for producing high performance concrete [4]. It has been reported that silica fume in concrete/mortar is an efficient pozzolanic material which results in more impermeable pore structure when compared to plain cement paste [5]. Addition of silica fume enhances the rate of cement hydration in early hours due to release of OH^- ions and alkalis in the pore fluids. Silica fume accelerates both C_3S and C_3A hydration during the first few hours [6]. It enables to provide nucleating sites to hydration products like lime, calcium silicate hydrates (CSH) and ettringite. Silica fume tends to affect the pattern of crystallization and degree of orientation of CH crystals at the aggregate surface during the first few days of hydration [7]. CSH plays a vital role in influencing the characteristics of cement paste. The compressive strength of cement paste decreases as the silica fume content increases at low w/b ratios (0.25) after 28 days [6]. At higher w/b ratio (0.45), with 30% silica fume the pastes exhibit higher strength at any age.

Hydration proceeds faster in pastes with silica fume, due to both $Ca(OH)_2$ and non-evaporable water contents at the early ages of 3 and 7 days. However, the hydration reactions in mortar terminate earlier. After 28 days, the non-evaporable water-content continues to increase significantly in plain cement concrete. The non-evaporable water content decreases between 90 and 550 days [8]. The optimum silica fume content to achieve higher strengths seems to range between 15 and 20%. Sabir reported that the strength development in concrete with condensed silica fume (CSF) is higher in the range of 12–28% [9]. The following three mechanisms: (1) strength enhancement by pore size refinement and matrix densification, (2) strength enhancement by reduction in content of $Ca(OH)_2$(CH), and (3) strength enhancement by cement paste-aggregate interfacial refinement, are believed to be responsible for the strength development of concrete and mortars containing silica fume [6].

TEST PROGRAM

Casting and Testing of Specimens

The materials used for casting specimens were OPC confirming to IS: 12269-1987, natural river sand having a fineness modulus of 2.67, machine-crushed granite with a maximum size of 19 mm, potable water and steel fibers of diameter 0.53 mm and length 25 mm. The SF used in this work was procured from Fosroc Chemicals India Pvt. Ltd., Bangalore, and the GP used in this work was obtained from Vasavi Granite Polishing Industry, Ongole. SF concrete, on account of larger surface area of fine products needs higher water content for same workability and so in order to limit the water content, superplasticizer has been added. Conplast SP:430 (Fosroc Chemicals) at 1% by weight of cement was added for the SF concrete. Three series of specimens, namely, (1) OPC series, (2) (OPC + SF) series in which 10% of the cement was replaced by SF, and (3) (OPC + GP) series where 10% of the cement was replaced by GP were casted with a constant water binder (w/b) ratio of 0.45. The mix proportions of concrete and specimen details for each series are given in Table 1. The specimen's both shear and flexure were casted and tested after curing in water for 28 days.

***Table 1**: Mix Proportions and Specimen Details.*

S. No.	Mix details by weight (Binder:sand:coarse aggregate)	w/b ratio	V_f (%)	No. of samples		No. of cylinders
				Shear	Flexure	
1.	1:2:3	0.45	0.0	3	3	6
2.	1:2:3	0.45	0.5	3	3	6
3.	1:2:3	0.45	1.0	3	3	6
4.	1:2:3	0.45	1.5	3	3	6

***Note:** Same for all the series.*

The constituent materials were thoroughly mixed in a machine mixer of 0.141 m^3 capacity to obtain a uniform mix. Fibers were added to the mixture at the very end to ensure that proper fiber dispersion was achieved and care was exercised to avoid balling of fibers. Fresh concrete was poured in steel molds and externally vibrated for proper compaction. From each mixture, the following specimens were cast: three 150 × 150 × 500 mm prisms for direct shear tests, three 150 × 150 × 650 mm beams for finding flexural toughness and six 100 mm diameter and 200 mm long cylinders for compressive strength and split-tensile strength. Central notches of 2 mm width and 75 mm long were formed in the flexure specimens of size 150 × 150 × 650 mm while casting. After 24 h of casting, the specimens were demolded and placed in water for curing up to the age of 28 days. After curing, the specimens were air-dried in shade before testing.

Testing of Specimens

Shear Tests

Two 15 mm-deep all-round notches to predefine the crack plane were cut in shear specimens as shown in Figure 1 using a diamond saw cutter [1]. Shear tests were conducted as per the JSCE SF-6 standard test method (Figure 2) [3]. In this test, the shear load was applied by a loading block with two sharp loading knife edges 150 mm apart. The beam was supported on another rigid block over a pair of knife edges that were 155 mm apart. Thus a 2.5 mm-wide region of the beam in-between the loading and the supporting knife edges was subjected to a concentrated shear stress, where shear failure was expected to occur.

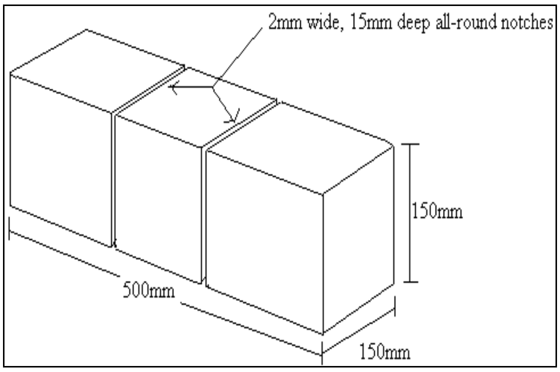

***Fig. 1:** Proposed Shear Test Specimen.*

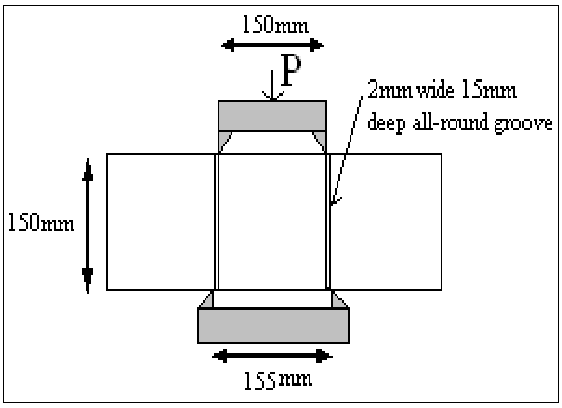

***Fig. 2:** Direct Shear Test Setup.*

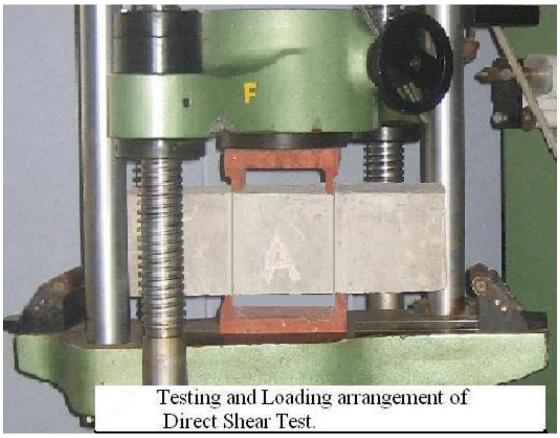

***Fig. 3**: Testing and Loading Arrangement of Direct Shear Test.*

Testing of specimens and loading arrangement are shown in Figure 3. The specimens were tested in a calibrated stiff 400 kN Universal Testing Machine (UTM) under load control. During testing, the slip was measured with the help of dial gages of 0.01 mm least count apart from the load-slip curves obtained directly from the machine with the help of a plotter.

Flexure Tests

The three-point bend (TPB) beam tests were conducted on flexure specimens of size 150 × 150 × 650 mm with an effective span of 600 mm so that span-to-depth ratio, l/d, is equal to 4.0 as per RILEM 50-FMC recommendations [10]. This standard test method is based on determining the amount of energy required to deflect and crack an SFRC beam loaded at mid-span with a central notch of a/d ratio 0.5. A typical TPB beam specimen is shown in Figure 4. Testing and loading arrangement is shown in Figure 5. A calibrated stiff 400kN UTM was used for testing of the specimens.

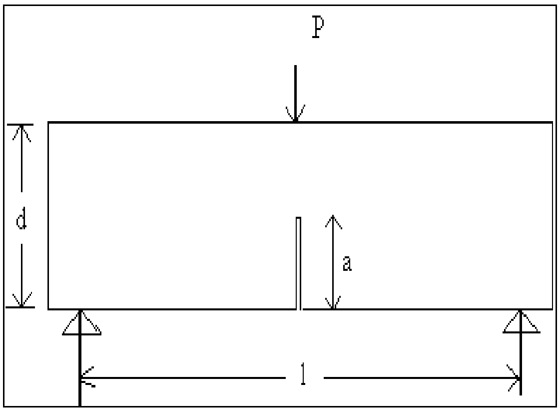

***Fig. 4:** A Typical TPB Beam Specimen.*

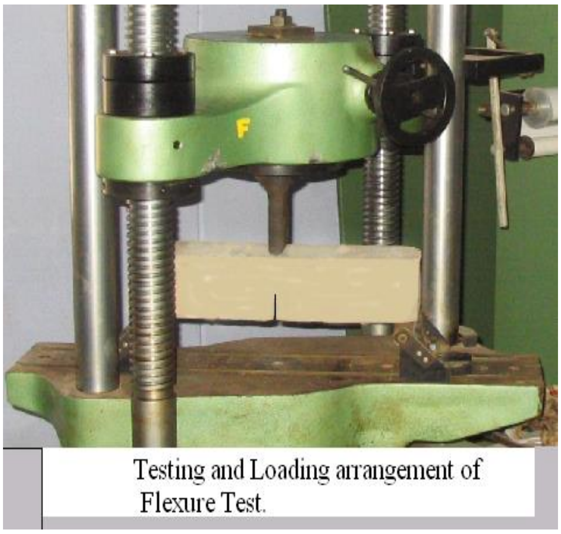

***Fig. 5:** Testing and Loading Arrangement of Flexure Test.*

Uniaxial Compression and Splitting Tension Tests

In order to find the compressive strength of concrete, three standard cylinders from each concrete series were tested under direct (uniaxial) compression. Three more cylinders from each series were tested for split-tensile strength according to IS: 5816-1999 in the above mentioned UTM [11].

RESULTS AND DISCUSSIONS

Failure Pattern of the Specimens

Figure 6 shows the tested specimens of plain and fiber reinforced concrete. It demonstrates that the failure of the specimens exhibited pure Mode II failure along the predetermined plane coinciding with the pre-notches.

Cylinder Compressive and Split-Tensile Strengths

A marginal increase in the cylinder compressive strength was observed with the addition of steel fibers. From results presented in Table 2, it is observed that the cylinder compressive strength is more or less constant for all the specimens. The results of the split-tensile strength of specimens are also presented in Table 2. From the results, it is clear that the fibers are very effective in increasing the split-tensile strength. A maximum of 31.3, 34.13, and 34.66% increase in the split-tensile strength was observed with the addition of fibers in OPC, (OPC + SF) and (OPC + GP) series respectively.

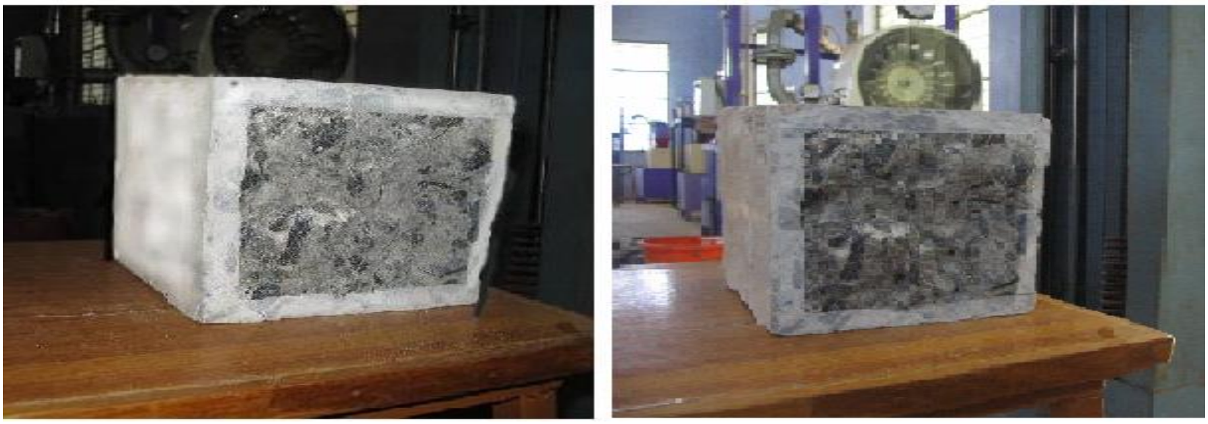

Fig. 6: *Tested Specimens of Proposed Direct Shear Test.*

Table 2*: Mechanical Properties of OPC, (OPC + SF) and (OPC + GP) Series.*

Concrete series	S. No.	Peak load 'P_{max}' (kN)	Max. slip 'δ_{max}' (mm)	f_c (MPa)	f_t (Mpa)
OPC	1	98.0	0.77	21.0	1.79
	2	118.0	8.50	21.4	2.19
	3	135.0	9.75	22.0	2.31
	4	150.0	10.8	22.0	2.35
OPC + SF	1	124.0	0.63	30.0	2.9
	2	148.0	8.67	30.3	3.62
	3	165.0	10.0	29.9	3.78
	4	183.0	10.6	29.7	3.89
OPC + GP	1	73.33	0.6	19.5	1.50
	2	88.0	7.75	20.0	1.89
	3	101.0	9.0	20.5	1.96
	4	110.0	11.0	20.0	2.02

The addition of silica fume increases the compressive strength of concrete whereas the addition of granite powder decreases the compressive strength. The percentage increase in the compressive strength of silica fume concrete over plain concrete is given in Table 3. An increase of about 38.78% in (OPC + SF) concretes has been observed. There has been decrease in compressive strength of concrete with the addition of granite powder. The percentage decrease in the compressive strength of GP concrete over plain concretes is presented in Table 3. A decrease of about 7.4% in (OPC + GP) concretes has been observed. Therefore, the addition of 10% granite powder as cement replacement material is found to be not favorable in strength improvement.

Table 3: *Percentage Increase in Compressive, Split-Tensile and Shear Strengths of (OPC + SF) and (OPC + GP) Series.*

Concrete series	S. No.	% Increase in f_c over OPC series	% Increase in f_t over OPC series
OPC + SF	1	42.86	62.0
	2	41.35	65.3
	3	35.90	63.64
	4	35.00	65.53
OPC + GP	1	−16.2	−16.2
	2	−13.7	−13.7
	3	−15.15	−15.15
	4	−14.04	−14.04

Note: *'− ' indicates decrease*

The split-tensile strength of concrete increases with the addition of silica fume, whereas it decreases with the addition of granite powder. The percentage changes of the strength with the addition of various cement replacement materials are also presented in Table 3. An increase of about 64.12% in (OPC + SF) concretes has been observed. A decrease of about 14.77% in (OPC + GP) concretes has been observed. The similar trends have also been reported by the earlier researchers [5, 9, 12–14].

Load-Slip Variations

Typical load-slip curves under direct shear loading for all the specimens tested for OPC, (OPC + SF) and (OPC + GP) series with different volume fraction of steel fibers are shown in Figures 7(a) to 7(d), Figures 8(a) to 8(d) and Figures 9(a) to 9(d) respectively. It demonstrates that the proposed method is capable of characterizing FRC under shear loading. The load-slip curves are linear up to the first cracking load, then tend to become nonlinear up to the peak load followed by a sudden drop and then are nearly horizontal exhibiting significant ductile behavior.

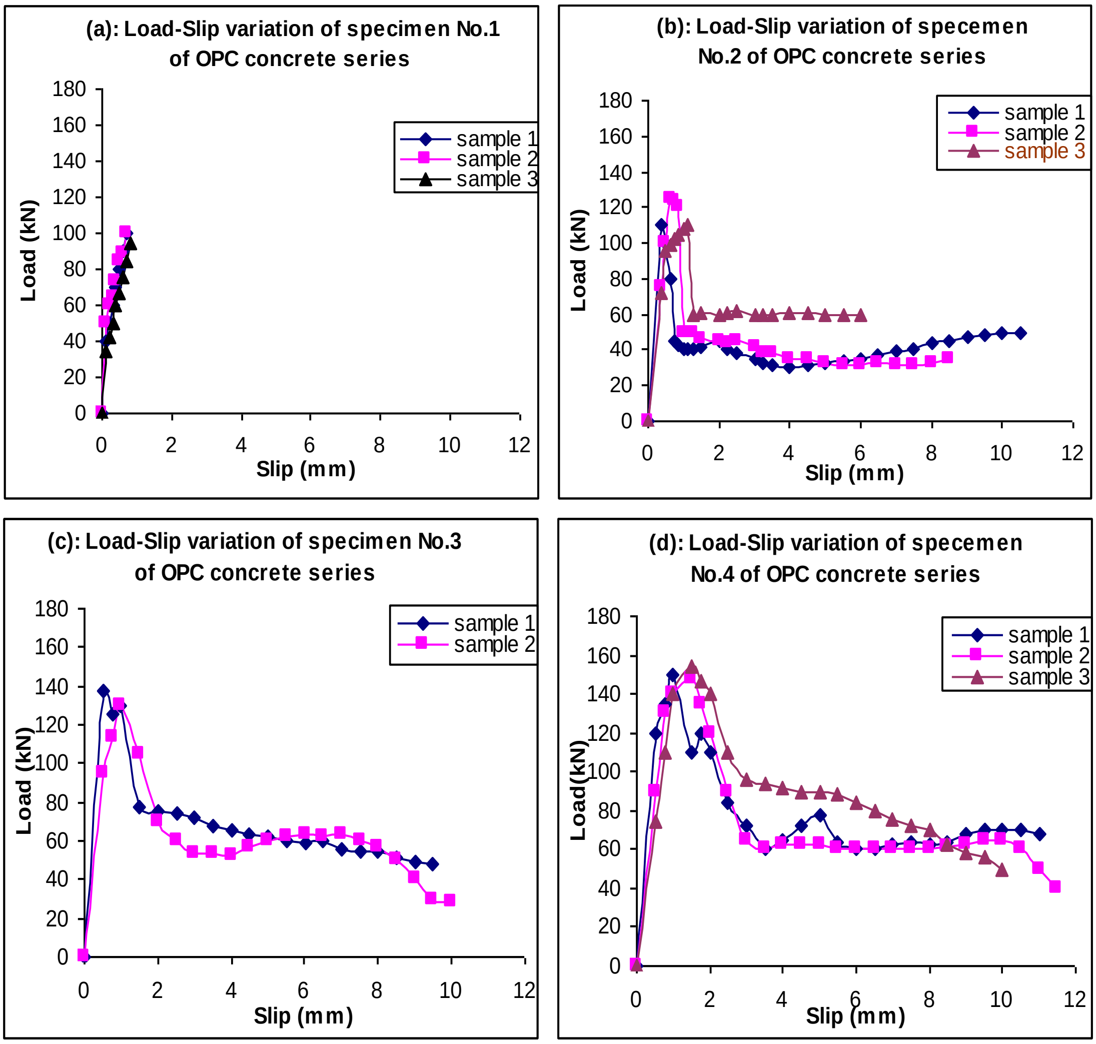

Fig. 7: *Load-Slip Variations in OPC Series.*

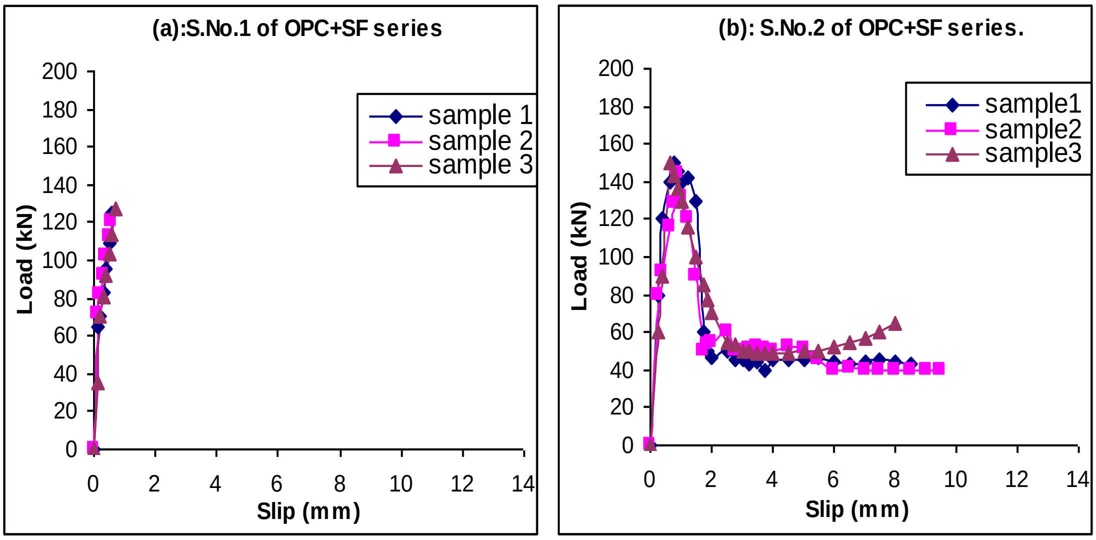

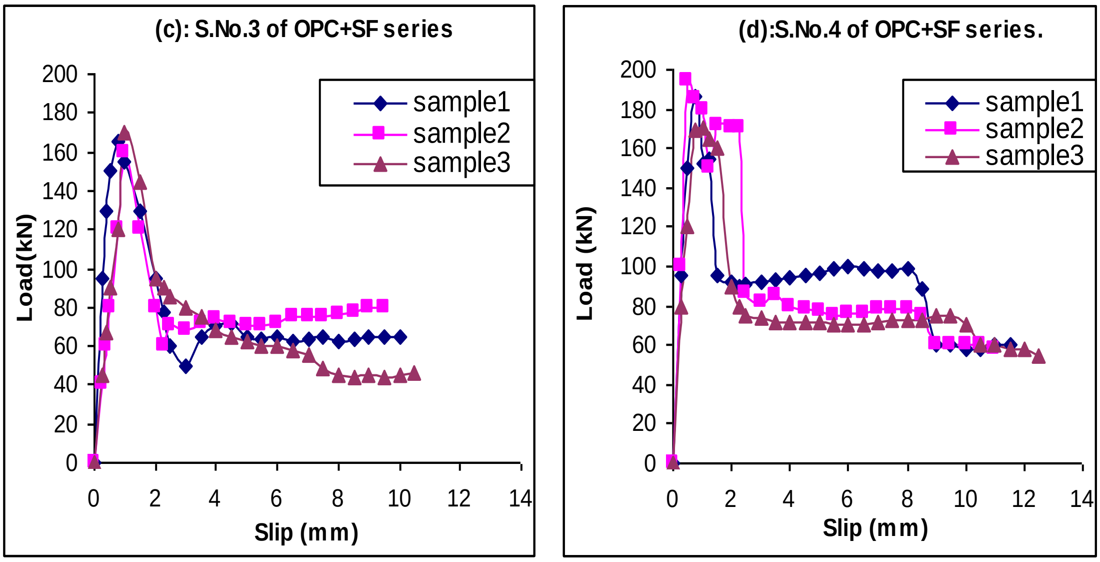

Fig. 8: *Load-Slip Variations in (OPC + SF) Series.*

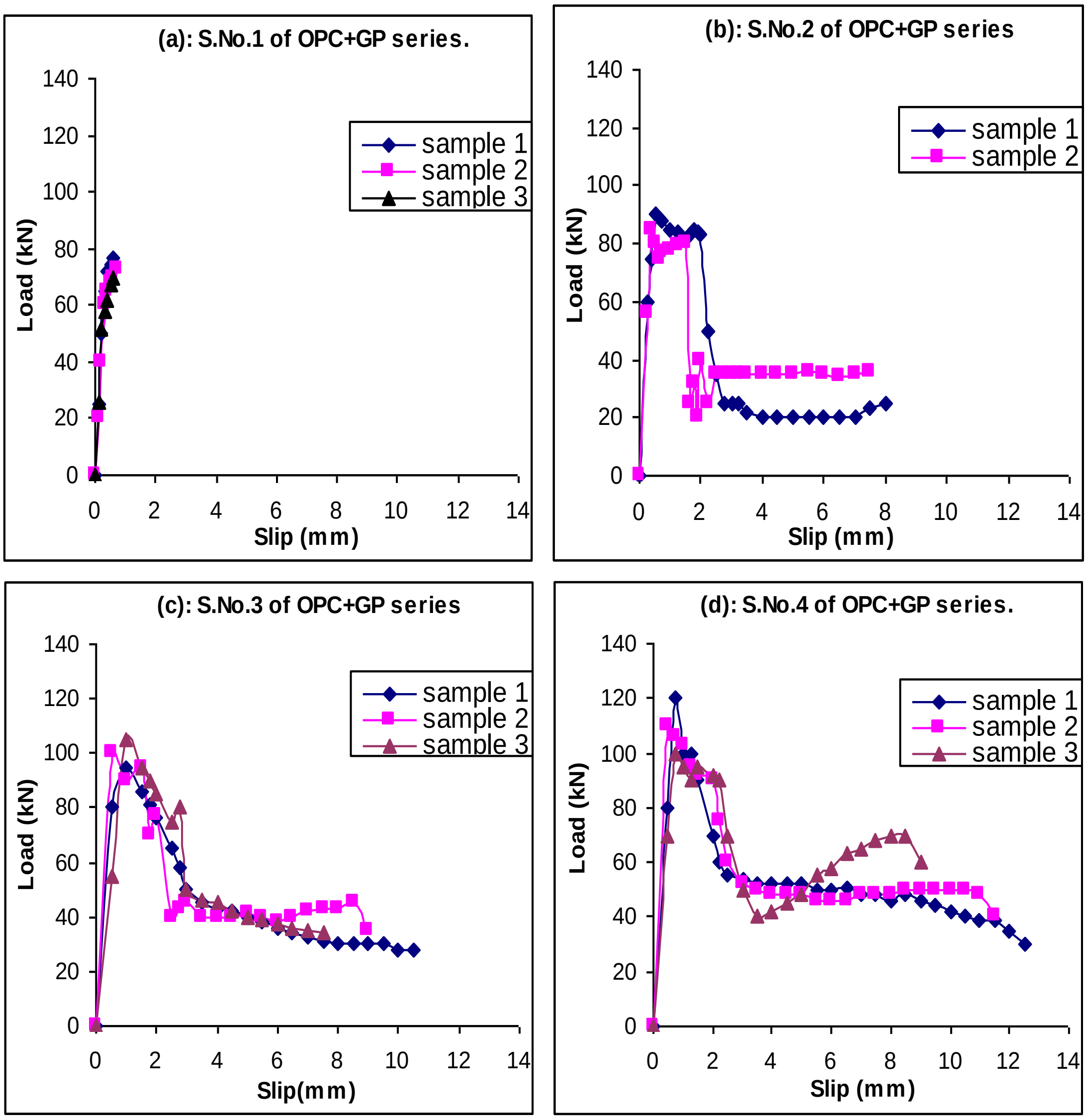

Fig. 9: *Load-Slip Variations in (OPC + GP) Series.*

Fracture Energy

The area under the load-slip curves was calculated, which is called work of fracture. In this case, it may be defined as shear toughness W_{Fs}. Then fracture energy per unit area in Mode II, G_{II} was computed using the formula,

$$G_{II} = W_{Fs}/(2A_{eff}) \quad (1)$$

where A_{eff} is the effective area of cross section of the specimen.

Table 4: *Fracture Properties of OPC, (OPC + SF) and (OPC + GP) Series.*

Concrete series	S. No	W_{Fs} (N−m)	W_{Ff} (N−m)	G_I (N/mm)	G_{II} (N/mm)
OPC	1	44		–	1.53
	2	446	12	1.067	15.49
	3	668	15	1.333	23.19
	4	885	22	1.955	30.73
OPC + SF	1	48		–	1.67
	2	512	14	1.24	17.78
	3	761	20	1.77	26.42
	4	1000	26	2.31	34.7
OPC + GP	1	32		–	1.09
	2	315	9.5	0.85	10.94
	3	501	12.5	1.11	17.39
	4	653	18.0	1.60	22.67

It has been observed that the fracture energy per unit cracking area, G_{II}, increases significantly with the addition of steel fibers. It has been further noticed that the fracture toughness increases as the volume fraction of fibers in the concrete increases. The effect of silica fume on various fracture parameters has been very positive. In other words, the addition of silica fume increases the fracture energy and fracture toughness in various concretes having incorporated with various volume fractions of steel fibers. However, the effect of granite powder in concretes has been observed to be different. The fracture energy and fracture toughness have been observed to decrease with the addition of granite powder. This could be explained by the following reasons. As the silica fume has a significant effect on the strength development at different ages of concrete, silica fume increases the bond strength between the fiber surface and the mortar matrix due to formation of strong interface between these two phases. Due to the micro-filling effect and also due to very high pozzolanic action of silica fume, it fills the gaps and refines the voids and vacancies with continuous reaction between various compounds with time. This results in very dense hardened concrete as the age of concrete increases.

The effect of silica fume and also the addition of steel fibers enhance the strength as well as ductility of the composite material. The addition of granite powder has not shown any improvement of the fracture properties of concrete. The granite powder simply acts as a filler material without any pozzolanic action on the strength development at any age. The increase/decrease in fracture properties of concretes are presented in Table 5. An average increase of about 12.70% in fracture energy, G_{II} in (OPC + SF) concretes has been observed in Mode II. An average decrease in fracture energy of about 27.33% in (OPC + GP) concretes has been observed.

Table 5: *Percentage Increase in Fracture Properties of (OPC + SF) and (OPC + GP) Series.*

Concrete series	S. No.	% Increase in G_I over OPC series	% Increase in G_{II} over OPC series
OPC + SF	1	–	9.15
	2	16.21	14.78
	3	20.04	13.93
	4	18.16	12.92
OPC + GP	1	–	−28.76
	2	−20.34	−29.37
	3	−16.73	−25.0
	4	−18.16	−26.2

Note: *'−' indicates decrease.*

Though the decrease in compressive strength of concrete with the addition of granite powder is about 7 to 8%, the decrease in fracture toughness in Mode II failure has been found to be about 15%. This change could be due to the decrease in bond strength between the mortar matrix and the steel fibers and also the coarse aggregate particles.

Shear Toughness versus Flexural Toughness

The test methods and the load-deflection plots of Mode I fracture are well established. However, for illustration purpose the typical load-deflection response of specimen No. 4 of OPC series in flexure is shown in Figure 10. The fracture toughness in Mode I was computed for all the specimens and is presented in Table 4. From the test results, it has been observed that the Mode II fracture energy is about 15 times greater than the Mode I fracture energy. Different from the flexure (Mode I) crack propagation, the shear (Mode II) crack propagation is in company with the compression failure after the maximum load. It could be due to the combined action of shear, compression and aggregate interlocking. Hence, the Mode II fracture energy is much more than Mode I fracture energy.

The fracture energy in Mode I loading, G_I, increases with the addition of silica fume, whereas it decreases with the addition of granite powder. The percentage increase or decrease in these values is also presented in Table 5. An increase of about 18.14% in (OPC + SF) concretes and decrease in Mode I fracture energy values of about 18.41% in (OPC + GP) concretes has been observed. Similar trends have been observed by Sabir [12]. From the results presented in Table 6, the ratio of G_{II} to G_I has been found to be 14.76 for (OPC + SF), 14.24 for (OPC + GP) and 15.88 for OPC series. Hence, for all the concrete specimens tested in this study, the ratio of G_{II} to G_I has been observed to be around 15.

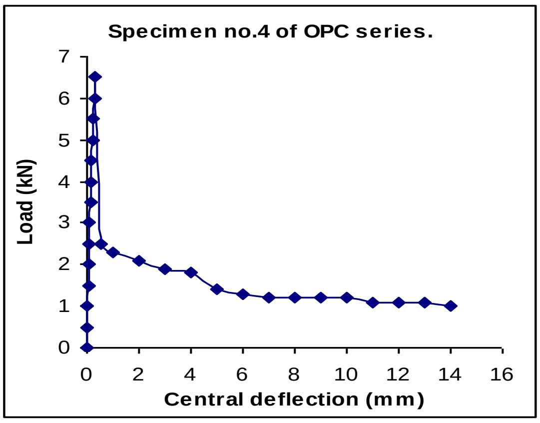

Fig. 10: *Load-Deflection Curve of S. No. 4 of OPC in TPB Beam Specimen.*

Table 6: *G_{II}/G_I Ratios in Different Concrete Series.*

S. No.	V_f (%)	OPC series	OPC + SF series	OPC + GP series
1	0.0	–	–	–
2	0.5	14.52	14.34	12.87
3	1.0	17.4	14.93	15.67
4	1.5	15.72	15.02	14.17

CONCLUSIONS

From the crack pattern, it has been observed that the failure planes are vertical indicating a predominant Mode II fracture. The steel fibers in plain concrete significantly improved the shear fracture energy as well as the flexure fracture energy in both the series. However, higher values have been observed with increase in the fiber volume fraction. An average increase of about 12.7% in Mode II fracture energy, G_{II}, has been observed in (OPC + SF) over OPC. An increase of about 18.14% in Mode I fracture energy, G_I, has also been observed in (OPC + SF) over OPC. An average decrease of about 27.33% in Mode II fracture energy, G_{II}, has been observed in (OPC + GP) over OPC. A decrease of about 18.41% in Mode I fracture energy, G_I, has also been observed in (OPC + GP) over OPC. The experimental results show that the ratio of Mode II to Mode I fracture energy is about 15 for all concretes tested in the study. Hence, the silica fume and granite powder have no effect on the ratio of Mode II to Mode I fracture energies.

REFERENCES

1. Appa Rao G, Rao AS. Toughness indices of fiber reinforced concrete subjected to mode II loading. *Proceedings of FraMCoS-7*, Korea Concrete Institute, Seoul. May 23–28, 2010; 112–117p. ISBN 978-89-5708-180-8.
2. Sreenivasa Rao A, Appa Rao G, Seshagiri Rao MV. Fracture behaviour and toughness of fiber reinforced concrete under Mode II loading. *Journal of Structural Engineering*. June-July 2009; 36(2): 141–7p.
3. JSCE SF-6. *Method of Test for Shear Strength of Steel Fiber Reinforced Concrete*. Japan Society of Civil Engineers, Tokyo. 1990; 67–9p.
4. Neville A, Aitcin PC. High performance concrete – An overview. *Materials and Structures*. 1998; 31: 111–7p.
5. Bayasi Z, Zhou J. Properties of silica fume concrete and mortar. *ACI Materials Journal*. 1993; 90(4): 349–56p.
6. Cheng Y, Feldman RF. Influence of silica fume on the micro-structural developments in cement mortars. *Cement*

and Concrete Research. 1985; 15(2): 285–94p.
7. Larbi JA, Fraay ALA, Bijen JMJM. The chemistry of the pore fluid of silica fume-blended cement systems. *Cement and Concrete Research*. 1990; 20(4): 506–16p.
8. Zhang MH, Gjorv OE. Effect of silica fume on cement hydration in low porosity cement pastes. *Cement Concrete Research.* 1991; 21(5): 800–8p.
9. Sabir BB. Strength and fracture toughness of silica fume concrete. *Magazine of Concrete Research*. 1997; 49(179): 139–46p.
10. RILEM Draft Recommendations. 50-FMC: Committee on fracture mechanics of concrete. *Materials and Structures*. 1985; 18(106): 285–90p.
11. IS: 5816-1999. Method of test for splitting tensile strength of concrete cylinders. *Bureau of Indian Standards.* New Delhi.
12. Swamy RN. Concrete Technology and Design. *Cement Replacement Materials*. 1986; 3.
13. Apparao G. Nonlinear fracture and size effect in high strength and high performance concrete: An experimental approach. *Ph.D. Thesis.* (Unpublished), IISc., Bangalore, 2001; 225–6p.
14. Sabir BB. Toughness and tortuosity of polypropylene fiber reinforced concrete. *Magazine of Concrete Research.* 2001; 53(3): 163–70p.

NOTATIONS

A_{eff} : Effective area of cross section
E : Young's modulus of elasticity of concrete
G_I : Fracture energy in Mode I per unit cracking area
G_{II} : Fracture energy in Mode II per unit cracking area
P_{max} : Peak load
V_f : Volume fraction of fibers
W_{Fs} : Shear toughness (work of fracture in shear)
W_{Ff} : Flexural toughness (work of fracture in flexure)
f_c : Cylinder compressive strength of concrete
f_t : Split-tensile strength of concrete
δ_{max} : Maximum slip

